

Enhancement of gravitational waves at Q-ball decay including non-linear density perturbations

Masahiro Kawasaki^{a,b} and Kai Murai^c

^aICRR, University of Tokyo, Kashiwa, 277-8582, Japan

^bKavli IPMU (WPI), UTIAS, University of Tokyo, Kashiwa, 277-8583, Japan

^cDepartment of Physics, Tohoku University, Sendai, 980-8578, Japan

E-mail: kawasaki@icrr.u-tokyo.ac.jp, kai.murai.e2@tohoku.ac.jp

Abstract. The existence of a stochastic gravitational wave background is indicated by the recent pulsar timing array (PTA) experiments. We study the enhanced production of second-order gravitational waves from the scalar perturbations when the universe experiences a transition from the early matter-dominated era to the radiation-dominated era due to Q-ball decay. We extend the analysis in previous work by including the frequency range where density perturbations go non-linear and find that the resultant gravitational wave spectrum can be consistent with that favored by the recent PTA experiment results.

Keywords: physics of the early universe, primordial gravitational waves (theory), supersymmetry and cosmology

Contents

1	Introduction	1
2	Q-ball scenario	2
3	Gravitational wave generation in the Q-ball scenario	4
3.1	Scalar perturbations	4
3.2	Second-order gravitational waves	7
4	Summary and Discussion	11

1 Introduction

Recently, the pulsar timing array (PTA) experiments, NANOGrav [1], EPTA [2] with InPTA data, PPTA [3], and CPTA [4], have reported the signal of a stochastic gravitational wave background in the nHz range. While it may indicate inspiring supermassive black holes [5–11], various possibilities for its origin have been discussed such as cosmic strings [12–22], domain walls [16, 23–35], a first-order phase transition [36–50], second-order effects of scalar perturbations [51–72], primordial tensor perturbations [73–81], and other scenarios [82–90]. See also Refs. [91–99] for model comparison.

The existence of the scalar perturbations has been confirmed through the cosmic microwave background (CMB) and large-scale structure observations. On the other hand, the primordial tensor perturbations have not been discovered on the CMB scales. In addition to the quantum fluctuations during inflation, the tensor perturbations can be sourced by the second-order effects of the scalar perturbations. In particular, if the universe experiences a matter-dominated era that suddenly transits to the standard radiation-dominated era, the scalar perturbations start to oscillate at the transition, and then gravitational waves can be abundantly generated [100]. This effect is called the “poltergeist effect”.

The poltergeist effect has been studied in various contexts such as PBH evaporation [65, 71, 101–107], Q-ball decay [108, 109], oscillon decay [110], and axion dynamics [111]. Among them, we studied the poltergeist effect in the Q-ball decay linking to lepton asymmetry generation [112] motivated by the recent determination of the primordial helium abundance [113, 114]. In Ref. [109], we included the effect of the finite decay rate and pointed out that the generated gravitational waves can be probed by the future PTA experiment, SKA.

Previous works on the poltergeist effect have been limited in the frequency range due to non-linear density perturbations in a high-frequency region. However, we naturally expect that gravitational waves are significantly generated in such a region. In this paper, we extend the analysis of the poltergeist effect using the fitting formula for non-linear density perturbations obtained from N -body simulations. Even if the density perturbations exceed unity and become non-linear, the gravitational potential, which sources the gravitational waves, is related to the density perturbation through the Poisson equation and can remain linear. By extending the frequency range, we find that the gravitational waves enhanced due to the Q-ball decay can be consistent with those favored by the PTA experiments and within reach of future experiments.

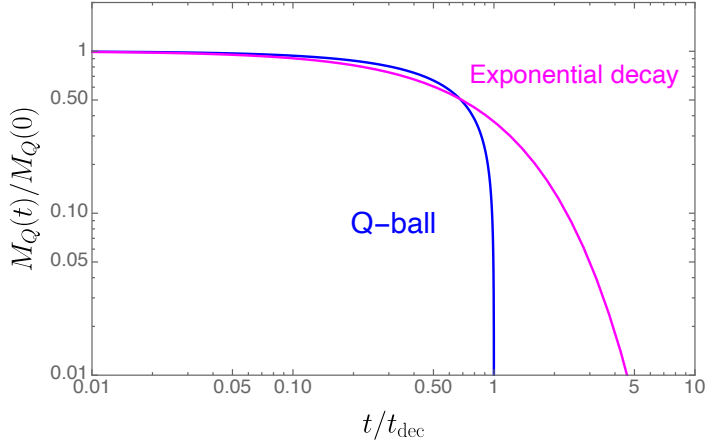


Figure 1. Evolution of a Q-ball mass (blue) compared to the exponential decay (magenta) given by $M_Q(t) = M_Q(0) \exp(-t/t_{\text{dec}})$.

The rest of this paper is organized as follows. In Sec. 2, we briefly review the Q-ball scenario generating the lepton asymmetry mainly focusing on Q-ball decay. The evolution of the scalar perturbations and production of gravitational waves in the Q-ball scenario including the non-linear regime are studied in Sec. 3. Our results are summarized and discussed in Sec. 4.

2 Q-ball scenario

First, we briefly review the Q-ball scenario following Refs. [109, 112]. A Q-ball is a non-topological soliton often formed in the Affleck-Dine (AD) mechanism in the minimal supersymmetric standard model (MSSM) [115, 116]. In the AD mechanism, a flat direction with a global U(1) charge (= baryon or lepton number) starts to oscillate with a velocity in the phase direction and generates the charge in the early universe. Depending on the shape of the scalar potential, the flat direction can fragment into spherical objects called Q-balls, which is classically stable due to the conservation of the U(1) charge [117–121]. Then, most of the charge generated in the AD mechanism is confined in the Q-balls. In this paper, we focus on a delayed-type Q-ball [122].

Depending on the type of Q-ball and the U(1) charge that Q-balls carry, Q-balls can decay and release their charge. For example, Q-balls with lepton charge decay emitting neutrinos. In this case, the mass of each delayed-type Q-ball, M_Q , evolves as

$$M_Q(t) = M_Q(0) \left(1 - \frac{t}{t_{\text{dec}}}\right)^{3/5}, \quad (2.1)$$

where t is the cosmic time, and $t = 0$ corresponds to the Q-ball formation. $t_{\text{dec}}(\propto M_Q(0)^{5/3})$ is the decay time, whose proportionality constant is determined by the model parameters. In Fig. 1, we show the evolution of the Q-ball mass following Eq. (2.1) and that in the case of the exponential decay for comparison. In the Q-ball decay, M_Q decreases faster than the exponential decay, which is important for the poltergeist effect.

Since Q-balls behave as non-relativistic matter, they can dominate the universe until their decay. In Fig. 2, we show the time evolution of the energy densities of the inflaton, radiation from the inflaton decay, Q-balls, radiation from the Q-ball decay, and non-relativistic

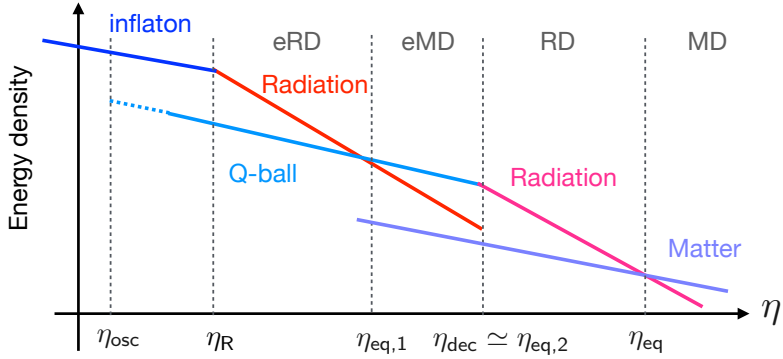


Figure 2. Evolution of the energy densities of the inflaton, radiation from the inflaton decay, Q-balls, radiation from the Q-ball decay, and non-relativistic matter in our scenario. η_{osc} denotes the conformal time when the AD field starts oscillations. η_{R} represents the completion of the reheating. $\eta_{\text{eq},1}$ and $\eta_{\text{eq},2}$ are the conformal times at matter-radiation equality between radiation and Q-balls. η_{eq} is the standard matter-radiation equality time.

matter in our scenario. The time coordinate is written in terms of the conformal time, η . Just after the decay of the inflaton, the universe is dominated by radiation, which we call the early radiation-dominated (eRD) era. Then, the Q-balls increase their energy fraction and come to have the energy density equal to that of radiation at $\eta = \eta_{\text{eq},1}$. From then, the universe is in the early matter-dominated (eMD) era, which ends around the Q-ball decay at $\eta = \eta_{\text{dec}}$. We denote the equality time around the Q-ball decay by $\eta_{\text{eq},2}$, which is approximately equal to η_{dec} . Then, the standard radiation-dominated (RD) era succeeds in for $\eta > \eta_{\text{eq},2}$, which is followed by the standard matter-dominated (MD) era for $\eta > \eta_{\text{eq}}$.

Now, we are interested in the enhancement of the second-order gravitational waves sourced by the scalar perturbations around the transition from the eMD era to the RD era. To evaluate the second-order gravitational waves, we parameterize the relevant properties of the Q-balls by two quantities: the decay temperature T_{dec} corresponding to t_{dec} or η_{dec} and the energy density ratio r_{dec} of the Q-balls to radiation at $T = T_{\text{dec}}$. The decay temperature is related to the corresponding wavenumber that reenters the horizon at $T = T_{\text{dec}}$ as

$$k_{\text{dec}} \equiv a_{\text{dec}} H_{\text{dec}} = 1.16 \times 10^4 \text{ Mpc}^{-1} \frac{T_{\text{dec}}}{1 \text{ MeV}}, \quad (2.2)$$

where we assumed $g_*(T_{\text{dec}}) = g_{*s}(T_{\text{dec}}) = 10.75$ and used $g_*(T_{\text{eq}}) = 2 + 21/4 \times (4/11)^{4/3}$, $g_{*s}(T_{\text{eq}}) = 43/11$, $a_{\text{eq}} H_{\text{eq}} = 0.0103 \text{ Mpc}^{-1}$ [123], and $T_{\text{eq}} = 3400 \times 2.725 \text{ K}$. On the other hand, the energy density ratio, r_{dec} , determines the duration of the eMD era through $\eta_{\text{dec}}/\eta_{\text{eq},1} \sim \sqrt{r_{\text{dec}}}$. For example, $T_{\text{dec}} = \mathcal{O}(1-10) \text{ MeV}$ and $r_{\text{dec}} = \mathcal{O}(10^7)$ are obtained in Ref. [112] while they are not the unique values to explain the lepton number generation.

In the eMD and RD eras ($\eta_{\text{eq},1} \leq \eta < \eta_{\text{eq}}$), the scale factor, a , and conformal Hubble

parameter, \mathcal{H} , are given respectively by

$$\frac{a(\eta)}{a(\eta_{\text{eq},1})} = \begin{cases} \left(\frac{\eta}{\eta_*}\right)^2 + \frac{2\eta}{\eta_*} & (\eta \leq \eta_{\text{dec}}) \\ \frac{2\eta(\eta_{\text{dec}} + \eta_*) - \eta_{\text{dec}}^2}{\eta_*^2} & (\eta > \eta_{\text{dec}}) \end{cases}, \quad (2.3)$$

$$\mathcal{H}(\eta) \equiv \frac{1}{a(\eta)} \frac{da(\eta)}{d\eta} = \begin{cases} \frac{2(\eta + \eta_*)}{\eta_*^2 + 2\eta\eta_*} & (\eta \leq \eta_{\text{dec}}) \\ \frac{1}{\eta - \frac{\eta_{\text{dec}}^2}{2(\eta_{\text{dec}} + \eta_*)}} & (\eta > \eta_{\text{dec}}) \end{cases}, \quad (2.4)$$

where $\eta_* \equiv \eta_{\text{eq},1}/(\sqrt{2} - 1)$. Here, we assumed sudden transitions at $\eta_{\text{eq},1}$ and $\eta_{\text{dec}} \simeq \eta_{\text{eq},2}$.

3 Gravitational wave generation in the Q-ball scenario

In this section, we discuss the enhancement of the second-order gravitational waves around the transition from the eMD era to the RD era. To this end, we first consider the evolution of the gravitational potential and then evaluate the sourced gravitational waves.

3.1 Scalar perturbations

Here, we discuss the evolution of the gravitational potential around the eMD era. We adopt the conformal Newtonian gauge and consider the metric perturbations given by

$$ds^2 = a^2 \left[-(1 + 2\Phi)d\eta^2 + \left((1 - 2\Psi)\delta_{ij} + \frac{1}{2}h_{ij} \right) dx^i dx^j \right], \quad (3.1)$$

where Φ and Ψ are scalar perturbations, and h_{ij} is tensor perturbations. In the early universe, we can neglect the anisotropic stress and obtain $\Phi = \Psi$.¹ To evaluate the production of gravitational waves, the evolution of the gravitational potential, Φ , is a key ingredient. Thus, we focus on the behavior of the transfer function, \mathcal{T} , of Φ around the eMD era. In particular, we discuss three effects: the transition from the eRD era to the eMD era, that from the eMD era to the RD era, and the non-linear evolution of the density perturbations during the eMD era. While the first two effects have been discussed in previous work [101, 109], the last one is the new effect that we first include in this paper.

First, we consider the transition from the eRD era to the eMD era. Around this transition, it is sufficient to discuss the scalar perturbations in the linear regime. In the eMD era, the gravitational potential becomes constant in the linear regime as in the standard MD era. We express this constant value of the transfer function by $\mathcal{T}_{\text{plateau}}$. While Φ on superhorizon scales at the transition is not suppressed at the transition, Φ on subhorizon scales at the transition is suppressed during the eRD era. The fitting formula of $\mathcal{T}_{\text{plateau}}$ is given

¹The anisotropic stress may be produced when the density perturbations go non-linear. Here we assume that the induced anisotropic stress is negligible.

by [101, 124]

$$\begin{aligned} \mathcal{T}_{\text{plateau}}(x_{\text{eq},1}) &\equiv \mathcal{T}(x)|_{\eta_{\text{eq},1} \ll \eta \lesssim \eta_{\text{dec}}} \\ &\simeq \frac{\ln[1 + 0.146x_{\text{eq},1}]}{0.146x_{\text{eq},1}} \\ &\quad \times \left[1 + 0.242x_{\text{eq},1} + (1.01x_{\text{eq},1})^2 + (0.341x_{\text{eq},1})^3 + (0.418x_{\text{eq},1})^4 \right]^{-1/4}, \end{aligned} \quad (3.2)$$

where $x_{\text{eq},1} \equiv k\eta_{\text{eq},1}$ and $x \equiv k\eta$ with k being the wavenumber of Φ . Note that, here, we normalize $\mathcal{T}_{\text{plateau}}$ so that $\mathcal{T}_{\text{plateau}}(x_{\text{eq},1} \rightarrow 0) \rightarrow 1$. In the limit of $x_{\text{eq},1} \gg 1$, the constant value is suppressed as $\mathcal{T}_{\text{plateau}}(x_{\text{eq},1} \gg 1) \propto x_{\text{eq},1}^{-2} \ln x_{\text{eq},1}$.

Next, we consider the transition from the eMD era to the RD era. Around this transition, \mathcal{T} decays proportionally to the matter density perturbations at first. In this phase, \mathcal{T} approximately decays as [125]

$$\frac{\mathcal{T}(t)}{\mathcal{T}_{\text{eMD}}} \simeq \frac{M_Q(t)}{M_{Q,\text{init}}} \simeq \left(1 - \frac{t}{t_{\text{dec}}} \right)^{3/5}, \quad (3.3)$$

where \mathcal{T}_{eMD} is the transfer function just before the Q-ball decay. While $\mathcal{T}_{\text{eMD}} = \mathcal{T}_{\text{plateau}}$ in the linear regime, it can be different from $\mathcal{T}_{\text{plateau}}$ if the density perturbations become non-linear as discussed below. The time evolution of Eq. (3.3) assumes that $\Phi(\propto \mathcal{T})$ is determined only by the matter density fluctuation, which requires

$$3a^2|\ddot{\mathcal{T}}| \ll k^2\mathcal{T} \quad (3.4)$$

$$\Leftrightarrow \frac{18}{25(t_{\text{dec}} - t)^2} \ll \frac{k^2}{a^2}, \quad (3.5)$$

as a necessary condition. Once this condition is violated, Φ decouples from the matter density perturbations and starts to independently oscillate.² To quantify this effect, we define the suppression factor of \mathcal{T} at the onset of oscillations by S satisfying $S(k) = \mathcal{T}_{\text{eMD}}$ in the sudden decay limit. From $\eta a = 3t$ during the eMD era, we obtain the decoupling time η_{dcpl} for a given k as

$$k\eta_{\text{dec}} - k\eta_{\text{dcpl}} \simeq \frac{9\sqrt{2}}{5}, \quad (3.6)$$

which leads to the lower bound of S , S_{low} , given by

$$S_{\text{low}} \simeq \left(\frac{9\sqrt{2}}{5k\eta_{\text{dec}}} \right)^{3/5} \mathcal{T}_{\text{eMD}} \equiv S_{\text{dec}} \mathcal{T}_{\text{eMD}}. \quad (3.7)$$

Here, S_{dec} denotes the suppression around the transition from the eMD era to the RD era. Note that this estimate of S_{dec} uses the equation of motion for Φ in the linear regime, and how the gravitational potential in the non-linear regime decays is non-trivial. However, Eq. (3.3) is derived from the Poisson equation, which is expected to be valid even in the non-linear

²Since Eq. (3.5) is a necessary condition, Φ can decouple from the matter density perturbations even before this condition is violated. Thus, the violation of Eq. (3.5) gives a lower bound for \mathcal{T} .

regime. Furthermore, as the Q-ball decay proceeds, the non-linearity decreases, which may partly justify the use of Eqs. (3.4) and (3.5). Therefore, in the following, we assume that the estimate above can also be applied to the non-linear regime.

After the gravitational potential decouples from the matter density fluctuation, the transfer function in the RD era follows the equation of

$$\mathcal{T}'' + 4\mathcal{H}\mathcal{T}' + \frac{k^2}{3}\mathcal{T} = 0, \quad (3.8)$$

where the primes denote the derivatives with respect to η . We can obtain \mathcal{T} after the decoupling by solving this equation with the approximated initial conditions, $\mathcal{T}(x_{\text{dec}} \equiv k\eta_{\text{dec}}) = S_{\text{low}}(k)$ and $\mathcal{T}'(x_{\text{dec}}) = 0$.

Finally, we discuss the non-linear evolution of the scalar perturbations. For simplicity, in this paper, we adopt the scale-invariant spectrum for the primordial curvature perturbations:

$$\mathcal{P}_\zeta(k) = C^2 A_s, \quad (3.9)$$

where $A_s = 2.1 \times 10^{-9}$ is the amplitude of the power spectrum on the CMB pivot scale $k_* = 0.05 \text{ Mpc}^{-1}$ [123]. Here, we introduced a constant C because we are focusing on scales much smaller than the CMB scale, and \mathcal{P}_ζ can be larger than A_s on such scales. For $k \gtrsim 10^5 \text{ Mpc}^{-1}$, the curvature perturbation is bounded as $\mathcal{P}_\zeta < \mathcal{O}(10^{-2})$ ($C < \mathcal{O}(10^3)$) from the PBH formation [126].

During the eMD era, the gravitational potential is almost constant in the linear regime. The linear density perturbation, $\delta_{\text{m,L}}$, can be evaluated from the Poisson equation as

$$\frac{3}{5}k^2\mathcal{T}_{\text{plateau}}(x_{\text{eq},1})\mathcal{P}_\zeta^{1/2} = \frac{3}{2}\mathcal{H}^2\delta_{\text{m,L}}(k), \quad (3.10)$$

where the factor of 3/5 comes from the relation between the gravitational potential and the curvature perturbation during the eMD era, $\Phi = (3/5)\mathcal{T}\zeta$. Since $\mathcal{H} \propto a^{-1/2}$ in the eMD era, the density perturbation grows as $\delta_{\text{m,L}} \propto a$. As a result, the density perturbation becomes non-linear during the eMD era for large k .

Once the density perturbation becomes non-linear, the evolution in the linear regime is no longer applicable, and the gravitational potential evolves in time. From the N -body simulations, the non-linear density fluctuation, $\delta_{\text{m,NL}}$ can be related to the linearly extrapolated density fluctuations $\delta_{\text{m,L}}$ using a function f_{NL} as [127, 128]

$$\delta_{\text{m,NL}}^2(k_{\text{NL}}) = f_{\text{NL}}[\delta_{\text{m,L}}^2(k_{\text{L}})], \quad (3.11)$$

where k_{L} is related to k_{NL} as

$$k_{\text{L}} = [1 + \delta_{\text{m,NL}}^2(k_{\text{NL}})]^{-1/3} k_{\text{NL}}. \quad (3.12)$$

In this paper, we adopt a fitting formula of f_{NL} given in Ref. [128]:³

$$f_{\text{NL}}(x) = x \left[\frac{1 + 0.4x + 0.498x^4}{1 + 0.00365x^3} \right]^{1/2}. \quad (3.13)$$

³There are more recent results on the non-linear evolution of the density perturbations such as Refs. [129–134]. However, they mainly focus on the power spectrum for the red-tilted curvature perturbations or that in the Λ CDM model. Now, we are interested in the non-linear evolution of the density perturbations for a scale-invariant \mathcal{P}_ζ in the matter-dominated universe. Thus, we adopted the fitting formula in Ref. [128], which agrees with the result for the correlation function including the case with a scale-invariant curvature perturbations [127].

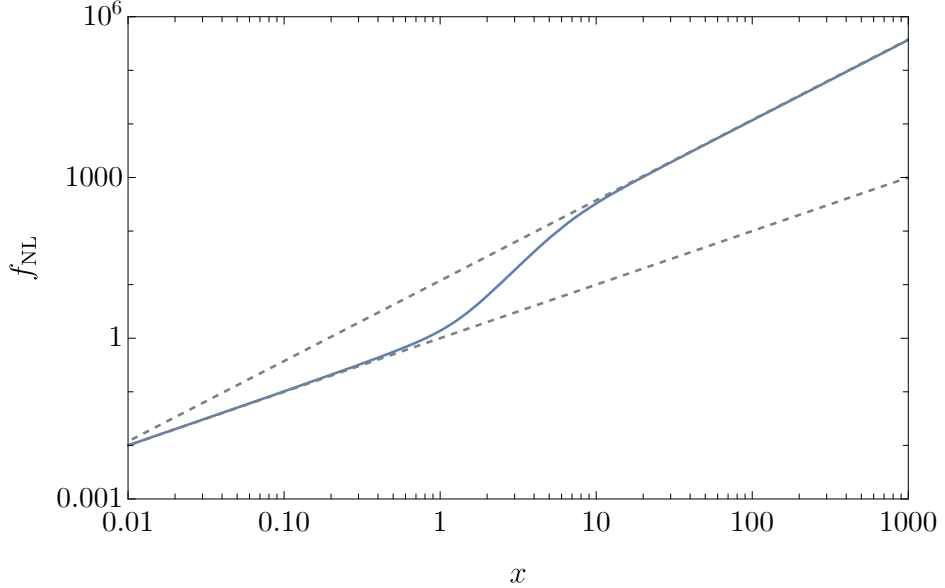


Figure 3. Fitting function of non-linear density perturbations, $f_{\text{NL}}(x)$. The upper and lower gray dashed lines denote $11.86x^{3/2}$ and x , respectively.

Since this formula is obtained from a fitting to N -body data, it can be inaccurate for the region where the fitted data is absent. In this paper, we consider that f_{NL} is reliable at least $f_{\text{NL}} < 10^3$ from the result in Ref. [127]. In the limit of $x \gg 1$, we obtain $f_{\text{NL}} \propto x^{3/2}$ while we obtain $f_{\text{NL}} \simeq x$ for $x \ll 1$. We can understand this dependency for $x \gg 1$ from $\delta_{\text{m,NL}}^2 \propto a^3$ in the stable clustering and $\delta_{\text{m,L}}^2 \propto a^2$ in the linear growth [127]. We show $f_{\text{NL}}(x)$ in Fig. 3. Even in the non-linear regime, the gravitational potential is related to the density fluctuation through the Poisson equation [135]. We define the correction factor of the gravitational potential in the non-linear regime compared to the linear solution, S_{NL} , by

$$\frac{3}{5}k^2 S_{\text{NL}}(k) \mathcal{T}_{\text{plateau}}(x_{\text{eq},1}) \mathcal{P}_\zeta^{1/2} = \frac{3}{2}\mathcal{H}^2 \delta_{\text{m,NL}}(k) . \quad (3.14)$$

Then, \mathcal{T}_{eMD} is represented as $\mathcal{T}_{\text{eMD}} = S_{\text{NL}} \mathcal{T}_{\text{plateau}}$. We show $S_{\text{NL}}(k)$ for $C = 30$ and several values of $\eta_{\text{dec}}/\eta_{\text{eq},1}$ in Fig. 4. While $f_{\text{NL}}(x) > x$ for all x as shown in Fig. 3, S_{NL} can be less than unity because f_{NL} relates the linear and non-linear density perturbations in different k (see Eqs. (3.11) and (3.12)). Incorporating S_{NL} , we define the correction factor for the gravitational potential due to the two transitions and non-linear effect, $S_{\text{low,NL}}$, by

$$S_{\text{low,NL}} \equiv S_{\text{dec}} S_{\text{NL}} \mathcal{T}_{\text{plateau}} . \quad (3.15)$$

3.2 Second-order gravitational waves

Next, we consider the generation of the second-order gravitational waves from the gravitational potential. We parameterize the gravitational wave energy density by the density parameter per $\ln k$ given by

$$\begin{aligned} \Omega_{\text{GW}}(\eta, k) &\equiv \frac{\rho_{\text{GW}}(\eta, k)}{\rho_{\text{tot}}(\eta)} \\ &= \frac{1}{24} \left(\frac{k}{a(\eta) H(\eta)} \right)^2 \overline{\mathcal{P}_h(\eta, k)} , \end{aligned} \quad (3.16)$$

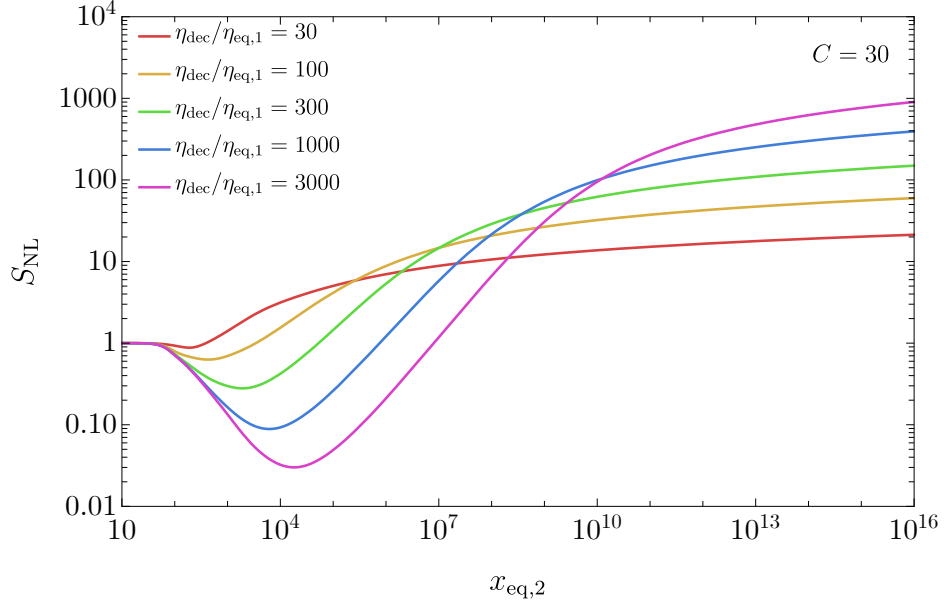


Figure 4. S_{NL} for $C = 30$ and $\eta_{\text{dec}}/\eta_{\text{eq},1} = 30, 100, 300, 1000$, and 3000 .

where ρ_{tot} is the total energy density at η , and $\overline{\mathcal{P}_h(\eta, k)}$ is the time average of the gravitational wave power spectrum. The power spectrum of the second-order gravitational waves is given by [136] (see also Refs. [137–142])

$$\overline{\mathcal{P}_h(\eta, k)} = 4 \int_0^\infty dv \int_{|1-v|}^{1+v} du \left[\frac{4v^2 - (1+v^2 - u^2)^2}{4vu} \right]^2 \overline{I^2(u, v, k, \eta, \eta_{\text{dec}})} \mathcal{P}_\zeta(uk) \mathcal{P}_\zeta(vk) , \quad (3.17)$$

where $I(u, v, k, \eta, \eta_{\text{dec}})$ is expressed as

$$I(u, v, k, \eta, \eta_{\text{dec}}) = \int_0^x d\tilde{x} \frac{a(\tilde{\eta})}{a(\eta)} k G_k(\eta, \tilde{\eta}) f(u, v, \tilde{x}, x_{\text{dec}}) , \quad (3.18)$$

with $\tilde{x} \equiv k\tilde{\eta}$. Here, $G_k(\eta, \tilde{\eta})$ is the Green function representing the propagation of the gravitational waves sourced at $\tilde{\eta}$ and satisfies

$$G_k''(\eta, \tilde{\eta}) + \left(k^2 - \frac{a''(\eta)}{a(\eta)} \right) G_k(\eta, \tilde{\eta}) = \delta(\eta - \tilde{\eta}) , \quad (3.19)$$

where the primes denote the derivatives with respect to not $\tilde{\eta}$ but η . $f(u, v, \tilde{x}, x_{\text{dec}})$ represents the second-order source term of the gravitational waves and is given by

$$\begin{aligned} f(u, v, \tilde{x}, x_{\text{dec}}) \\ \equiv \frac{3 [2(5 + 3w(\tilde{\eta})) \mathcal{T}(u\tilde{x}) \mathcal{T}(v\tilde{x}) + 4\mathcal{H}^{-1}(\mathcal{T}'(u\tilde{x}) \mathcal{T}(v\tilde{x}) + \mathcal{T}(u\tilde{x}) \mathcal{T}'(v\tilde{x})) + 4\mathcal{H}^{-2} \mathcal{T}'(u\tilde{x}) \mathcal{T}'(v\tilde{x})]}{25(1 + w(\tilde{\eta}))} , \end{aligned} \quad (3.20)$$

where $w(\tilde{\eta}) \equiv p/\rho$ is the equation-of-state parameter at $\tilde{\eta}$, and $\mathcal{T}(x)$ is an abbreviated notation of $\mathcal{T}(x, x_{\text{eq},1}, x_{\text{dec}})$. Note that the primes denote derivatives with respect to the conformal time as mentioned above, and thus $\mathcal{T}'(u\tilde{x}) = \partial\mathcal{T}(u\tilde{x})/\partial\tilde{\eta} = uk\partial\mathcal{T}(u\tilde{x})/\partial(u\tilde{x})$.

We evaluate the gravitational wave spectrum at a certain time, $\eta = \eta_c$, after the energy density of the gravitational waves becomes constant and before the late-time equality. Then, we translate it into the current energy density spectrum. Due to the resonance among the oscillations of the gravitational potentials in f and the Green function G_k , $\overline{\mathcal{P}_h}$ has a resonant contribution. In this paper, we focus on the dominant resonant contribution.

First, we review the evaluation with a cutoff of the scalar perturbations at $k = k_{\text{cut}}$, which is defined by $\delta_{\text{m,L}}(k_{\text{cut}}) = 1$ in Eq. (3.10). With this cutoff, the gravitational wave spectrum is estimated as [100, 101]

$$\Omega_{\text{GW,RD}}^{(\text{res})}(\eta_c, k) \simeq 2.9 \times 10^{-7} Y \mathcal{P}_\zeta^2 S_{\text{low}}^4(k) (k \eta_{\text{dec}})^7 F(s_0(k), n_{\text{s,eff}}) , \quad (3.21)$$

where $Y \simeq 2.3$ is the numerical fudge factor, and $F(s_0(k), n_{\text{s,eff}})$ reflects the effect of the cutoff at $k = k_{\text{cut}}$ in the wavenumber integration. $F(s_0(k), n_{\text{s,eff}})$ is defined by

$$\begin{aligned} & F(s, n_{\text{s,eff}}) \\ & \equiv 2s \left(\frac{3}{4} \right)^{n_{\text{s,eff}}-1} \\ & \times \left[4 {}_2F_1 \left(\frac{1}{2}, 1 - n_{\text{s,eff}}; \frac{3}{2}; \frac{s^2}{3} \right) - 3 {}_2F_1 \left(\frac{1}{2}, -n_{\text{s,eff}}; \frac{3}{2}; \frac{s^2}{3} \right) - s^2 {}_2F_1 \left(\frac{3}{2}, -n_{\text{s,eff}}; \frac{5}{2}; \frac{s^2}{3} \right) \right] , \end{aligned} \quad (3.22)$$

and

$$s_0(k) = \begin{cases} 1 & (k \leq \frac{2}{1+\sqrt{3}} k_{\text{cut}}) \\ \frac{2}{k} k_{\text{cut}} - \sqrt{3} & (\frac{2}{1+\sqrt{3}} k_{\text{cut}} \leq k \leq \frac{2}{\sqrt{3}} k_{\text{cut}}) \\ 0 & (k \geq \frac{2}{\sqrt{3}} k_{\text{cut}}) \end{cases} , \quad (3.23)$$

with ${}_2F_1$ being a hypergeometric function. Here, $n_{\text{s,eff}}$ represents the effective spectral index of the scalar perturbations including the suppression effects discussed above, $\mathcal{T}_{\text{plateau}}$ and S_{dec} . Note that this formula is obtained for a constant value of $n_{\text{s,eff}}$.

Next, we extend this formula to include the nonlinear regime, $k > k_{\text{cut}}$. Specifically, we eliminate the cutoff at k_{cut} and introduce S_{NL} . Since we do not set a cutoff of the scalar perturbations, we replace $s_0(k)$ by unity in Eq. (3.21). Considering the discussion in Sec. 3.1, we can decompose $n_{\text{s,eff}}$ into four contributions as

$$n_{\text{s,eff}} = n_s + \Delta n_{\text{s,plateau}} + \Delta n_{\text{s,dec}} + \Delta n_{\text{s,NL}} . \quad (3.24)$$

Here, $n_s = 1$ is the index of \mathcal{P}_ζ determined in Eq. (3.9), $\Delta n_{\text{s,plateau}}$ represents the momentum dependence of $\mathcal{T}_{\text{plateau}}$ and is given by

$$\Delta n_{\text{s,plateau}}(k) = 2 \frac{d \ln \mathcal{T}_{\text{plateau}}}{d \ln k} \simeq \begin{cases} 0 & (k \eta_{\text{eq},1} \ll 1) \\ -4 & (k \eta_{\text{eq},1} \gg 1) \end{cases} , \quad (3.25)$$

$\Delta n_{\text{s,dec}} = -6/5$ reflects the k -dependence of S_{dec} in Eq. (3.7), and $\Delta n_{\text{s,NL}}$ accounts for the non-linear evolution of Φ by

$$\Delta n_{\text{s,NL}}(k) = 2 \frac{d \ln S_{\text{NL}}}{d \ln k} . \quad (3.26)$$

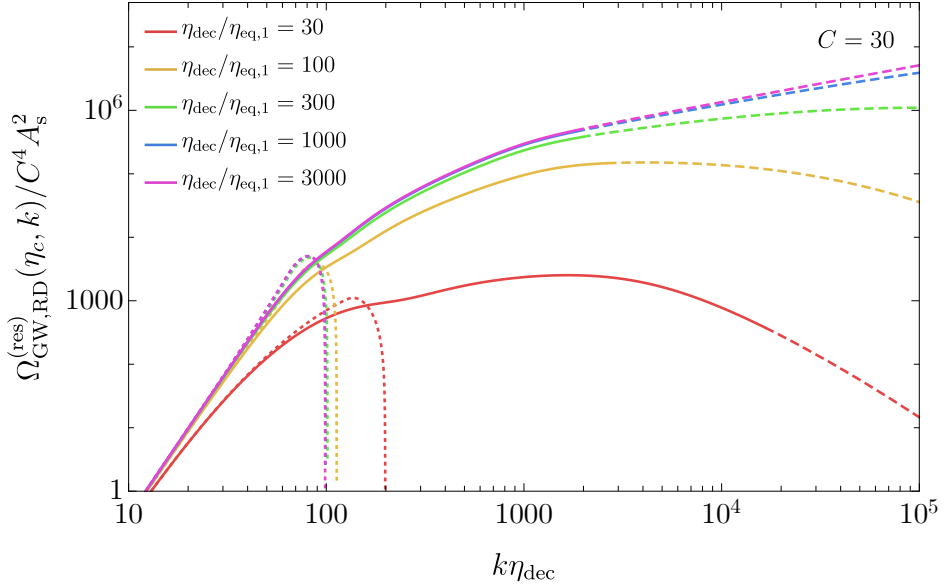


Figure 5. Shapes of the gravitational wave spectrum for different values of $\eta_{\text{dec}}/\eta_{\text{eq},1}$. Here, we fix $C = 30$. In the regions with dashed lines, the estimate of S_{NL} can be inaccurate. The dotted lines denote the gravitational wave spectrum from the linear scalar perturbations with the cutoff at $k = k_{\text{cut}}$.

Although the formula of Eq. (3.21) is obtained for a constant $n_{\text{s,eff}}$, we substitute the k -dependent $n_{\text{s,eff}}$ as a rough estimate. Then, we obtain the gravitational wave spectrum as

$$\Omega_{\text{GW, RD}}^{(\text{res})}(\eta_c, k) \simeq 2.9 \times 10^{-7} Y \mathcal{P}_\zeta^2 S_{\text{low, NL}}^4(k) (k\eta_{\text{dec}})^7 F(1, n_{\text{s,eff}}(k)) . \quad (3.27)$$

This formula still depends on η_{dec} and $\eta_{\text{eq},1}$, which are determined by T_{dec} and $\eta_{\text{dec}}/\eta_{\text{eq},1}$. Thus, we can evaluate $\Omega_{\text{GW, RD}}^{(\text{res})}$ for fixed values of T_{dec} , $\eta_{\text{dec}}/\eta_{\text{eq},1}$, and C . We show the shape of the gravitational wave abundance for $C = 30$ and different values of $\eta_{\text{dec}}/\eta_{\text{eq},1}$ in Fig. 5. The region where $\delta_{\text{m, NL}}^2(k) > 10^3$ is shown by dashed lines. For comparison, we also show the gravitational wave spectrum from the linear scalar perturbations with the cutoff at $k = k_{\text{cut}}$ by dotted lines.

Finally, we translate the gravitational wave energy density parameter during the RD era to that at the present time by [143]

$$\Omega_{\text{GW,0}}(k) h^2 = 0.83 \left(\frac{g_{*,c}}{10.75} \right)^{-1/3} \Omega_{\text{r,0}} h^2 \Omega_{\text{GW, RD}}^{(\text{res})}(\eta_c, k) , \quad (3.28)$$

where $g_{*,c}$ is the effective degrees of freedom at η_c , and $\Omega_{\text{r,0}}$ is the current density parameter of radiation. We use $g_{*,c} = 10.75$ and $\Omega_{\text{r,0}} h^2 = 4.2 \times 10^{-5}$. We show the current density parameter of the gravitational waves for $T_{\text{dec}} = 3$ MeV, $\eta_{\text{dec}}/\eta_{\text{eq},1} = 1000$, and $C = 30, 10, 300$ in Fig. 6. Again, the dotted lines represent the gravitational waves sourced by the scalar perturbations in the linear regime. The recent PTA data favor the signal for $T_{\text{dec}} = 3$ MeV, $\eta_{\text{dec}}/\eta_{\text{eq},1} = 1000$, and $C = 300$. Note that these values are not the only parameter set to match the PTA data. For instance, larger T_{dec} and C will also be favored by the data. In any case, we can see that the non-linear evaluation is crucial to compare the gravitational wave spectrum with the PTA data.

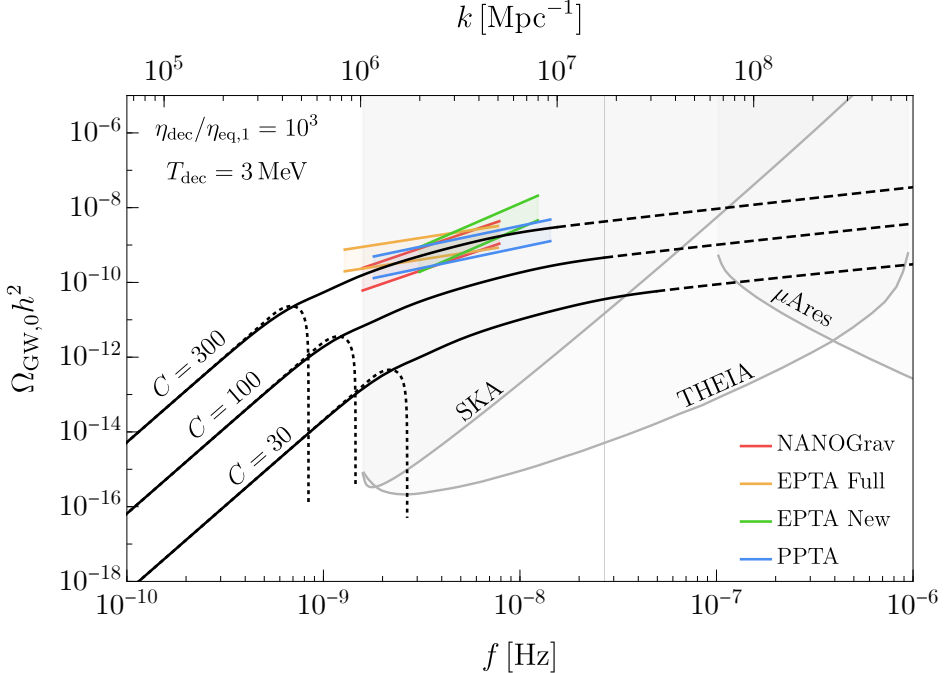


Figure 6. Current density parameter of the gravitational waves for $T_{\text{dec}} = 3 \text{ MeV}$ and $C = 30, 100$, and 300 from bottom to top. The dashed and dotted lines are used in the same way as in Fig. 5. We fix $\eta_{\text{dec}}/\eta_{\text{eq},1} = 1000$. The colored bands are the 95% regions for the best-fit tilt indicated by the recent PTA experiments, NANOGrav [1], EPTA [2] with InPTA data, and PPTA [3]. The frequency ranges are determined as the region where the signals seem to be inconsistent with the null hypothesis. The gray-shaded regions are the future sensitivities of SKA [144, 145], THEIA [146], and μ Ares [147]. The sensitivity of SKA is taken from Ref. [148]

4 Summary and Discussion

In this paper, we have extended the analysis for the Q-ball scenario in Ref. [109] and discussed the second-order gravitational waves sourced by the scalar perturbations including the non-linear regime. By using the fitting formula for the non-linear density perturbations, we could evaluate the gravitational wave spectrum for larger frequencies than previous work. The resultant gravitational wave spectrum depends on the properties of the Q-ball decay and primordial curvature perturbations. For a certain parameter set, which can be realized in the Q-ball scenario, the GW spectrum becomes consistent with the signal recently reported by the PTA experiments. Moreover, the Q-ball scenario is based on the MSSM framework, and gravitinos are produced after the reheating. After the dilution by the Q-ball decay, gravitinos can account for dark matter. In this sense, this scenario can simultaneously explain the primordial helium abundance, gravitational waves suggested by the PTA experiments, and dark matter.

Before closing the paper, we make some comments on the limitations of our analysis. Our result is the first step to evaluate the gravitational waves sourced by the scalar perturbations in the non-linear regime, and some improvements can be considered. First, our analysis adopts the estimate of S_{dec} obtained in the linear regime. In this sense, we expect that a more robust spectrum for a wider frequency range can be obtained with a deeper understanding of the non-linear dynamics through numerical investigation such as N -body simulations.

Second, the scalar perturbations in the non-linear regime become non-Gaussian through the growth. Since our evaluation of the sourced gravitational waves assumes the Gaussian properties of the gravitational potential, its non-Gaussianity will result in some correction in the gravitational wave spectrum.

Third, in this paper, we have assumed that all the Q-balls complete their decay at the same time. However, the decay process of the Q-balls can deviate in time due to fluctuations in the initial mass or formation time in a realistic situation. In this case, the universe experiences a more gradual transition from the eMD era to the RD era, which will suppress the gravitational waves as discussed in Ref. [101].

Finally, we have focused on the resonant gravitational waves sourced by the primordial curvature perturbations. The second-order gravitational waves also have non-resonant contributions. Although the non-resonant contribution is smaller than the resonant contribution around the non-linear scale, k_{cut} [100, 101], it will become non-negligible in lower frequency regions. In addition, we can also consider the density perturbation of Q-balls in analogy to the analysis in the PBH evaporation scenario [65, 102–107]. In the PBH scenario, such a contribution produces gravitational waves in a higher frequency region [104], which will also be true in our scenario. It will be interesting to study the detectability of such gravitational waves in interferometer experiments and the effects of non-linearity on this contribution, but it is out of the scope of this work.

Acknowledgments

We would like to thank Keisuke Inomata and Naoki Yoshida for their helpful comments. This work was supported by JSPS KAKENHI Grant Nos. 20H05851(M.K.), 21K03567(M.K.), and 23KJ0088(K.M.), and World Premier International Research Center Initiative (WPI Initiative), MEXT, Japan (M.K.).

References

- [1] NANOGrav collaboration, G. Agazie et al., *The NANOGrav 15 yr Data Set: Evidence for a Gravitational-wave Background*, *Astrophys. J. Lett.* **951** (2023) L8, [[2306.16213](#)].
- [2] EPTA collaboration, J. Antoniadis et al., *The second data release from the European Pulsar Timing Array III. Search for gravitational wave signals*, [2306.16214](#).
- [3] D. J. Reardon et al., *Search for an Isotropic Gravitational-wave Background with the Parkes Pulsar Timing Array*, *Astrophys. J. Lett.* **951** (2023) L6, [[2306.16215](#)].
- [4] H. Xu et al., *Searching for the Nano-Hertz Stochastic Gravitational Wave Background with the Chinese Pulsar Timing Array Data Release I*, *Res. Astron. Astrophys.* **23** (2023) 075024, [[2306.16216](#)].
- [5] NANOGrav collaboration, G. Agazie et al., *The NANOGrav 15 yr Data Set: Constraints on Supermassive Black Hole Binaries from the Gravitational-wave Background*, *Astrophys. J. Lett.* **952** (2023) L37, [[2306.16220](#)].
- [6] J. Ellis, M. Fairbairn, G. Hütsi, J. Raidal, J. Urrutia, V. Vaskonen et al., *Gravitational Waves from SMBH Binaries in Light of the NANOGrav 15-Year Data*, [2306.17021](#).
- [7] T. Broadhurst, C. Chen, T. Liu and K.-F. Zheng, *Binary Supermassive Black Holes Orbiting Dark Matter Solitons: From the Dual AGN in UGC4211 to NanoHertz Gravitational Waves*, [2306.17821](#).

- [8] P. F. Depta, K. Schmidt-Hoberg, P. Schwaller and C. Tasillo, *Do pulsar timing arrays observe merging primordial black holes?*, [2306.17836](#).
- [9] Y.-C. Bi, Y.-M. Wu, Z.-C. Chen and Q.-G. Huang, *Implications for the Supermassive Black Hole Binaries from the NANOGrav 15-year Data Set*, [2307.00722](#).
- [10] C. Zhang, N. Dai, Q. Gao, Y. Gong, T. Jiang and X. Lu, *Detecting new fundamental fields with Pulsar Timing Arrays*, [2307.01093](#).
- [11] E. Cannizzaro, G. Franciolini and P. Pani, *Novel tests of gravity using nano-Hertz stochastic gravitational-wave background signals*, [2307.11665](#).
- [12] J. Ellis, M. Lewicki, C. Lin and V. Vaskonen, *Cosmic Superstrings Revisited in Light of NANOGrav 15-Year Data*, [2306.17147](#).
- [13] Z. Wang, L. Lei, H. Jiao, L. Feng and Y.-Z. Fan, *The nanohertz stochastic gravitational-wave background from cosmic string Loops and the abundant high redshift massive galaxies*, [2306.17150](#).
- [14] N. Kitajima and K. Nakayama, *Nanohertz gravitational waves from cosmic strings and dark photon dark matter*, [2306.17390](#).
- [15] A. Eichhorn, R. R. Lino dos Santos and J. a. L. Miqueleto, *From quantum gravity to gravitational waves through cosmic strings*, [2306.17718](#).
- [16] G. Lazarides, R. Maji and Q. Shafi, *Superheavy quasi-stable strings and walls bounded by strings in the light of NANOGrav 15 year data*, [2306.17788](#).
- [17] G. Servant and P. Simakachorn, *Constraining Post-Inflationary Axions with Pulsar Timing Arrays*, [2307.03121](#).
- [18] S. Antusch, K. Hinze, S. Saad and J. Steiner, *Singling out $SO(10)$ GUT models using recent PTA results*, [2307.04595](#).
- [19] W. Buchmuller, V. Domcke and K. Schmitz, *Metastable cosmic strings*, [2307.04691](#).
- [20] M. Yamada and K. Yonekura, *Dark baryon from pure Yang-Mills theory and its GW signature from cosmic strings*, [2307.06586](#).
- [21] G. Lazarides, R. Maji, A. Moursy and Q. Shafi, *Inflation, superheavy metastable strings and gravitational waves in non-supersymmetric flipped $SU(5)$* , [2308.07094](#).
- [22] W. Ahmed, M. U. Rehman and U. Zubair, *Probing Stochastic Gravitational Wave Background from $SU(5) \times U(1)_\chi$ Strings in Light of NANOGrav 15-Year Data*, [2308.09125](#).
- [23] S.-Y. Guo, M. Khlopov, X. Liu, L. Wu, Y. Wu and B. Zhu, *Footprints of Axion-Like Particle in Pulsar Timing Array Data and JWST Observations*, [2306.17022](#).
- [24] N. Kitajima, J. Lee, K. Murai, F. Takahashi and W. Yin, *Nanohertz Gravitational Waves from Axion Domain Walls Coupled to QCD*, [2306.17146](#).
- [25] Y. Bai, T.-K. Chen and M. Korwar, *QCD-Collapsed Domain Walls: QCD Phase Transition and Gravitational Wave Spectroscopy*, [2306.17160](#).
- [26] S. Blasi, A. Mariotti, A. Rase and A. Sevrin, *Axionic domain walls at Pulsar Timing Arrays: QCD bias and particle friction*, [2306.17830](#).
- [27] Y. Gouttenoire and E. Vitagliano, *Domain wall interpretation of the PTA signal confronting black hole overproduction*, [2306.17841](#).
- [28] B. Barman, D. Borah, S. Jyoti Das and I. Saha, *Scale of Dirac leptogenesis and left-right symmetry in the light of recent PTA results*, [2307.00656](#).
- [29] B.-Q. Lu and C.-W. Chiang, *Nano-Hertz stochastic gravitational wave background from domain wall annihilation*, [2307.00746](#).

- [30] X. K. Du, M. X. Huang, F. Wang and Y. K. Zhang, *Did the nHz Gravitational Waves Signatures Observed By NANOGrav Indicate Multiple Sector SUSY Breaking?*, [2307.02938](#).
- [31] X.-F. Li, *Probing the high temperature symmetry breaking with gravitational waves from domain walls*, [2307.03163](#).
- [32] E. Babichev, D. Gorbunov, S. Ramazanov, R. Samanta and A. Vikman, *NANOGrav spectral index $\gamma = 3$ from melting domain walls*, [2307.04582](#).
- [33] G. B. Gelmini and J. Hyman, *Catastrogesis with unstable ALPs as the origin of the NANOGrav 15 yr gravitational wave signal*, [2307.07665](#).
- [34] S. Ge, *Stochastic gravitational wave background: birth from axionic string-wall death*, [2307.08185](#).
- [35] Z. Zhang, C. Cai, Y.-H. Su, S. Wang, Z.-H. Yu and H.-H. Zhang, *Nano-Hertz gravitational waves from collapsing domain walls associated with freeze-in dark matter in light of pulsar timing array observations*, [2307.11495](#).
- [36] L. Zu, C. Zhang, Y.-Y. Li, Y.-C. Gu, Y.-L. S. Tsai and Y.-Z. Fan, *Mirror QCD phase transition as the origin of the nanohertz Stochastic Gravitational-Wave Background*, [2306.16769](#).
- [37] C. Han, K.-P. Xie, J. M. Yang and M. Zhang, *Self-interacting dark matter implied by nano-Hertz gravitational waves*, [2306.16966](#).
- [38] E. Megias, G. Nardini and M. Quiros, *Pulsar Timing Array Stochastic Background from light Kaluza-Klein resonances*, [2306.17071](#).
- [39] K. Fujikura, S. Girmohanta, Y. Nakai and M. Suzuki, *NANOGrav Signal from a Dark Conformal Phase Transition*, [2306.17086](#).
- [40] A. Addazi, Y.-F. Cai, A. Marciano and L. Visinelli, *Have pulsar timing array methods detected a cosmological phase transition?*, [2306.17205](#).
- [41] Y. Xiao, J. M. Yang and Y. Zhang, *Implications of Nano-Hertz Gravitational Waves on Electroweak Phase Transition in the Singlet Dark Matter Model*, [2307.01072](#).
- [42] S.-P. Li and K.-P. Xie, *A collider test of nano-Hertz gravitational waves from pulsar timing arrays*, [2307.01086](#).
- [43] D. Wang, *Constraining Cosmological Phase Transitions with Chinese Pulsar Timing Array Data Release 1*, [2307.15970](#).
- [44] T. Ghosh, A. Ghoshal, H.-K. Guo, F. Hajkarim, S. F. King, K. Sinha et al., *Did we hear the sound of the Universe boiling? Analysis using the full fluid velocity profiles and NANOGrav 15-year data*, [2307.02259](#).
- [45] J. S. Cruz, F. Niedermann and M. S. Sloth, *NANOGrav meets Hot New Early Dark Energy and the origin of neutrino mass*, [2307.03091](#).
- [46] P. Di Bari and M. H. Rahat, *The split majoron model confronts the NANOGrav signal*, [2307.03184](#).
- [47] Y. Gouttenoire, *First-order Phase Transition interpretation of PTA signal produces solar-mass Black Holes*, [2307.04239](#).
- [48] A. Salvio, *Supercooling in Radiative Symmetry Breaking: Theory Extensions, Gravitational Wave Detection and Primordial Black Holes*, [2307.04694](#).
- [49] M. Ahmadvand, L. Bian and S. Shakeri, *A Heavy QCD Axion model in Light of Pulsar Timing Arrays*, [2307.12385](#).
- [50] H. An, B. Su, H. Tai, L.-T. Wang and C. Yang, *Phase transition during inflation and the gravitational wave signal at pulsar timing arrays*, [2308.00070](#).

[51] G. Franciolini, A. Iovino, Junior., V. Vaskonen and H. Veermae, *The recent gravitational wave observation by pulsar timing arrays and primordial black holes: the importance of non-gaussianities*, [2306.17149](#).

[52] Y.-F. Cai, X.-C. He, X. Ma, S.-F. Yan and G.-W. Yuan, *Limits on scalar-induced gravitational waves from the stochastic background by pulsar timing array observations*, [2306.17822](#).

[53] K. Inomata, K. Kohri and T. Terada, *The Detected Stochastic Gravitational Waves and Subsolar-Mass Primordial Black Holes*, [2306.17834](#).

[54] S. Wang, Z.-C. Zhao, J.-P. Li and Q.-H. Zhu, *Exploring the Implications of 2023 Pulsar Timing Array Datasets for Scalar-Induced Gravitational Waves and Primordial Black Holes*, [2307.00572](#).

[55] L. Liu, Z.-C. Chen and Q.-G. Huang, *Implications for the non-Gaussianity of curvature perturbation from pulsar timing arrays*, [2307.01102](#).

[56] R. Ebadi, S. Kumar, A. McCune, H. Tai and L.-T. Wang, *Gravitational Waves from Stochastic Scalar Fluctuations*, [2307.01248](#).

[57] K. T. Abe and Y. Tada, *Translating nano-Hertz gravitational wave background into primordial perturbations taking account of the cosmological QCD phase transition*, [2307.01653](#).

[58] Z. Yi, Q. Gao, Y. Gong, Y. Wang and F. Zhang, *The waveform of the scalar induced gravitational waves in light of Pulsar Timing Array data*, [2307.02467](#).

[59] Q.-H. Zhu, Z.-C. Zhao and S. Wang, *Joint implications of BBN, CMB, and PTA Datasets for Scalar-Induced Gravitational Waves of Second and Third orders*, [2307.03095](#).

[60] H. Firouzjahi and A. Talebian, *Induced Gravitational Waves from Ultra Slow-Roll Inflation and Pulsar Timing Arrays Observations*, [2307.03164](#).

[61] Z.-Q. You, Z. Yi and Y. Wu, *Constraints on primordial curvature power spectrum with pulsar timing arrays*, [2307.04419](#).

[62] S. A. Hosseini Mansoori, F. Felegray, A. Talebian and M. Sami, *PBHs and GWs from \mathbb{T}^2 -inflation and NANOGrav 15-year data*, [2307.06757](#).

[63] K. Cheung, C. J. Ouseph and P.-Y. Tseng, *NANOGrav Signal and PBH from the Modified Higgs Inflation*, [2307.08046](#).

[64] S. Balaji, G. Domènech and G. Franciolini, *Scalar-induced gravitational wave interpretation of PTA data: the role of scalar fluctuation propagation speed*, [2307.08552](#).

[65] S. Basilakos, D. V. Nanopoulos, T. Papanikolaou, E. N. Saridakis and C. Tzerefos, *Signatures of Superstring theory in NANOGrav*, [2307.08601](#).

[66] J.-H. Jin, Z.-C. Chen, Z. Yi, Z.-Q. You, L. Liu and Y. Wu, *Confronting sound speed resonance with pulsar timing arrays*, [2307.08687](#).

[67] B. Das, N. Jaman and M. Sami, *Gravitational Waves Background (NANOGrav) from Quintessential Inflation*, [2307.12913](#).

[68] Z.-C. Zhao, Q.-H. Zhu, S. Wang and X. Zhang, *Exploring the Equation of State of the Early Universe: Insights from BBN, CMB, and PTA Observations*, [2307.13574](#).

[69] L. Liu, Z.-C. Chen and Q.-G. Huang, *Probing the equation of state of the early Universe with pulsar timing arrays*, [2307.14911](#).

[70] Z. Yi, Z.-Q. You and Y. Wu, *Model-independent reconstruction of the primordial curvature power spectrum from PTA data*, [2308.05632](#).

[71] N. Bhaumik, R. K. Jain and M. Lewicki, *Ultra-low mass PBHs in the early universe can explain the PTA signal*, [2308.07912](#).

[72] S. Choudhury, A. Karde, S. Panda and M. Sami, *Scalar induced gravity waves from ultra slow-roll Galileon inflation*, [2308.09273](#).

[73] S. Vagnozzi, *Inflationary interpretation of the stochastic gravitational wave background signal detected by pulsar timing array experiments*, *JHEAp* **39** (2023) 81–98, [\[2306.16912\]](#).

[74] S. Datta, *Inflationary gravitational waves, pulsar timing data and low-scale-leptogenesis*, [2307.00646](#).

[75] D. Chowdhury, G. Tasinato and I. Zavala, *Dark energy, D-branes, and Pulsar Timing Arrays*, [2307.01188](#).

[76] S. Choudhury, *Single field inflation in the light of NANOGrav 15-year Data: Quintessential interpretation of blue tilted tensor spectrum through Non-Bunch Davies initial condition*, [2307.03249](#).

[77] M. A. Gorji, M. Sasaki and T. Suyama, *Extra-tensor-induced origin for the PTA signal: No primordial black hole production*, [2307.13109](#).

[78] I. Ben-Dayan, U. Kumar, U. Thattarampilly and A. Verma, *Probing The Early Universe Cosmology With NANOGrav: Possibilities and Limitations*, [2307.15123](#).

[79] J.-Q. Jiang, Y. Cai, G. Ye and Y.-S. Piao, *Broken blue-tilted inflationary gravitational waves: a joint analysis of NANOGrav 15-year and BICEP/Keck 2018 data*, [2307.15547](#).

[80] M. Zhu, G. Ye and Y. Cai, *Pulsar timing array observations as a possible hint for nonsingular cosmology*, [2307.16211](#).

[81] L. Frosina and A. Urbano, *On the inflationary interpretation of the nHz gravitational-wave background*, [2308.06915](#).

[82] J. Yang, N. Xie and F. P. Huang, *Implication of nano-Hertz stochastic gravitational wave background on ultralight axion particles*, [2306.17113](#).

[83] Y. Li, C. Zhang, Z. Wang, M. Cui, Y.-L. S. Tsai, Q. Yuan et al., *Primordial magnetic field as a common solution of nanohertz gravitational waves and Hubble tension*, [2306.17124](#).

[84] V. K. Oikonomou, *Flat energy spectrum of primordial gravitational waves versus peaks and the NANOGrav 2023 observation*, *Phys. Rev. D* **108** (2023) 043516, [\[2306.17351\]](#).

[85] D. Borah, S. Jyoti Das and R. Samanta, *Inflationary origin of gravitational waves with textitMiracle-less WIMP dark matter in the light of recent PTA results*, [2307.00537](#).

[86] K. Murai and W. Yin, *A Novel Probe of Supersymmetry in Light of Nanohertz Gravitational Waves*, [2307.00628](#).

[87] X. Niu and M. H. Rahat, *NANOGrav signal from axion inflation*, [2307.01192](#).

[88] C. Unal, A. Papageorgiou and I. Obata, *Axion-Gauge Dynamics During Inflation as the Origin of Pulsar Timing Array Signals and Primordial Black Holes*, [2307.02322](#).

[89] M. Geller, S. Ghosh, S. Lu and Y. Tsai, *Challenges in Interpreting the NANOGrav 15-Year Data Set as Early Universe Gravitational Waves Produced by ALP Induced Instability*, [2307.03724](#).

[90] P. Bari, N. Bartolo, G. Domènech and S. Matarrese, *Gravitational waves induced by scalar-tensor mixing*, [2307.05404](#).

[91] NANOGrav collaboration, A. Afzal et al., *The NANOGrav 15 yr Data Set: Search for Signals from New Physics*, *Astrophys. J. Lett.* **951** (2023) L11, [\[2306.16219\]](#).

[92] G. Lambiase, L. Mastrototaro and L. Visinelli, *Astrophysical neutrino oscillations after pulsar timing array analyses*, [2306.16977](#).

[93] G. Franciolini, D. Racco and F. Rompineve, *Footprints of the QCD Crossover on Cosmological Gravitational Waves at Pulsar Timing Arrays*, [2306.17136](#).

[94] L. Bian, S. Ge, J. Shu, B. Wang, X.-Y. Yang and J. Zong, *Gravitational wave sources for Pulsar Timing Arrays*, [2307.02376](#).

[95] D. G. Figueroa, M. Pieroni, A. Ricciardone and P. Simakachorn, *Cosmological Background Interpretation of Pulsar Timing Array Data*, [2307.02399](#).

[96] Y.-M. Wu, Z.-C. Chen and Q.-G. Huang, *Cosmological Interpretation for the Stochastic Signal in Pulsar Timing Arrays*, [2307.03141](#).

[97] G. Ye and A. Silvestri, *Can the gravitational wave background feel wiggles in spacetime?*, [2307.05455](#).

[98] Y. Cui, S. Kumar, R. Sundrum and Y. Tsai, *Unraveling Cosmological Anisotropies within Stochastic Gravitational Wave Backgrounds*, [2307.10360](#).

[99] J. Ellis, M. Fairbairn, G. Franciolini, G. Hütsi, A. Iovino, M. Lewicki et al., *What is the source of the PTA GW signal?*, [2308.08546](#).

[100] K. Inomata, K. Kohri, T. Nakama and T. Terada, *Enhancement of Gravitational Waves Induced by Scalar Perturbations due to a Sudden Transition from an Early Matter Era to the Radiation Era*, *Phys. Rev. D* **100** (2019) 043532, [[1904.12879](#)].

[101] K. Inomata, M. Kawasaki, K. Mukaida, T. Terada and T. T. Yanagida, *Gravitational Wave Production right after a Primordial Black Hole Evaporation*, *Phys. Rev. D* **101** (2020) 123533, [[2003.10455](#)].

[102] G. Domènech, C. Lin and M. Sasaki, *Gravitational wave constraints on the primordial black hole dominated early universe*, *JCAP* **04** (2021) 062, [[2012.08151](#)].

[103] G. Domènech, V. Takhistov and M. Sasaki, *Exploring evaporating primordial black holes with gravitational waves*, *Phys. Lett. B* **823** (2021) 136722, [[2105.06816](#)].

[104] N. Bhaumik, A. Ghoshal and M. Lewicki, *Doubly peaked induced stochastic gravitational wave background: testing baryogenesis from primordial black holes*, *JHEP* **07** (2022) 130, [[2205.06260](#)].

[105] T. Papanikolaou, *Gravitational waves induced from primordial black hole fluctuations: the effect of an extended mass function*, *JCAP* **10** (2022) 089, [[2207.11041](#)].

[106] N. Bhaumik, A. Ghoshal, R. K. Jain and M. Lewicki, *Distinct signatures of spinning PBH domination and evaporation: doubly peaked gravitational waves, dark relics and CMB complementarity*, *JHEP* **05** (2023) 169, [[2212.00775](#)].

[107] G. Domènech and M. Sasaki, *Gravitational wave hints black hole remnants as dark matter*, *Class. Quant. Grav.* **40** (2023) 177001, [[2303.07661](#)].

[108] G. White, L. Pearce, D. Vagie and A. Kusenko, *Detectable Gravitational Wave Signals from Affleck-Dine Baryogenesis*, *Phys. Rev. Lett.* **127** (2021) 181601, [[2105.11655](#)].

[109] S. Kasuya, M. Kawasaki and K. Murai, *Enhancement of second-order gravitational waves at Q-ball decay*, *JCAP* **05** (2023) 053, [[2212.13370](#)].

[110] K. D. Lozanov and V. Takhistov, *Enhanced Gravitational Waves from Inflaton Oscillons*, *Phys. Rev. Lett.* **130** (2023) 181002, [[2204.07152](#)].

[111] K. Harigaya, K. Inomata and T. Terada, *Axion Poltergeist*, [2305.14242](#).

[112] M. Kawasaki and K. Murai, *Lepton asymmetric universe*, *JCAP* **08** (2022) 041, [[2203.09713](#)].

[113] A. Matsumoto et al., *EMPRESS. VIII. A New Determination of Primordial He Abundance with Extremely Metal-poor Galaxies: A Suggestion of the Lepton Asymmetry and Implications for the Hubble Tension*, *Astrophys. J.* **941** (2022) 167, [[2203.09617](#)].

[114] A.-K. Burns, T. M. P. Tait and M. Valli, *Indications for a Nonzero Lepton Asymmetry from Extremely Metal-Poor Galaxies*, *Phys. Rev. Lett.* **130** (2023) 131001, [[2206.00693](#)].

[115] I. Affleck and M. Dine, *A New Mechanism for Baryogenesis*, *Nucl. Phys. B* **249** (1985) 361–380.

[116] M. Dine, L. Randall and S. D. Thomas, *Baryogenesis from flat directions of the supersymmetric standard model*, *Nucl. Phys. B* **458** (1996) 291–326, [[hep-ph/9507453](#)].

[117] S. R. Coleman, *Q-balls*, *Nucl. Phys. B* **262** (1985) 263.

[118] A. Kusenko, *Solitons in the supersymmetric extensions of the standard model*, *Phys. Lett. B* **405** (1997) 108, [[hep-ph/9704273](#)].

[119] A. Kusenko and M. E. Shaposhnikov, *Supersymmetric Q balls as dark matter*, *Phys. Lett. B* **418** (1998) 46–54, [[hep-ph/9709492](#)].

[120] K. Enqvist and J. McDonald, *Q balls and baryogenesis in the MSSM*, *Phys. Lett. B* **425** (1998) 309–321, [[hep-ph/9711514](#)].

[121] S. Kasuya and M. Kawasaki, *Q ball formation through Affleck-Dine mechanism*, *Phys. Rev. D* **61** (2000) 041301, [[hep-ph/9909509](#)].

[122] S. Kasuya and M. Kawasaki, *Q ball formation: Obstacle to Affleck-Dine baryogenesis in the gauge mediated SUSY breaking?*, *Phys. Rev. D* **64** (2001) 123515, [[hep-ph/0106119](#)].

[123] PLANCK collaboration, N. Aghanim et al., *Planck 2018 results. VI. Cosmological parameters*, *Astron. Astrophys.* **641** (2020) A6, [[1807.06209](#)].

[124] J. M. Bardeen, J. R. Bond, N. Kaiser and A. S. Szalay, *The Statistics of Peaks of Gaussian Random Fields*, *Astrophys. J.* **304** (1986) 15–61.

[125] K. Inomata, K. Kohri, T. Nakama and T. Terada, *Gravitational Waves Induced by Scalar Perturbations during a Gradual Transition from an Early Matter Era to the Radiation Era*, *JCAP* **10** (2019) 071, [[1904.12878](#)].

[126] A. D. Gow, C. T. Byrnes, P. S. Cole and S. Young, *The power spectrum on small scales: Robust constraints and comparing PBH methodologies*, *JCAP* **02** (2021) 002, [[2008.03289](#)].

[127] A. J. S. Hamilton, A. Matthews, P. Kumar and E. Lu, *Reconstructing the primordial spectrum of fluctuations of the universe from the observed nonlinear clustering of galaxies*, *Astrophys. J. Lett.* **374** (1991) L1.

[128] J. A. Peacock and S. J. Dodds, *Reconstructing the linear power spectrum of cosmological mass fluctuations*, *Mon. Not. Roy. Astron. Soc.* **267** (1994) 1020–1034, [[astro-ph/9311057](#)].

[129] H. J. Mo, B. Jain and S. D. M. White, *The Evolution of correlation functions and power spectra in gravitational clustering*, *Mon. Not. Roy. Astron. Soc.* **276** (1995) L25–L29, [[astro-ph/9501047](#)].

[130] J. A. Peacock and S. J. Dodds, *Nonlinear evolution of cosmological power spectra*, *Mon. Not. Roy. Astron. Soc.* **280** (1996) L19, [[astro-ph/9603031](#)].

[131] VIRGO CONSORTIUM collaboration, R. E. Smith, J. A. Peacock, A. Jenkins, S. D. M. White, C. S. Frenk, F. R. Pearce et al., *Stable clustering, the halo model and nonlinear cosmological power spectra*, *Mon. Not. Roy. Astron. Soc.* **341** (2003) 1311, [[astro-ph/0207664](#)].

[132] R. Takahashi, M. Sato, T. Nishimichi, A. Taruya and M. Oguri, *Revising the Halofit Model for the Nonlinear Matter Power Spectrum*, *Astrophys. J.* **761** (2012) 152, [[1208.2701](#)].

[133] A. Mead, J. Peacock, C. Heymans, S. Joudaki and A. Heavens, *An accurate halo model for fitting non-linear cosmological power spectra and baryonic feedback models*, *Mon. Not. Roy. Astron. Soc.* **454** (2015) 1958–1975, [[1505.07833](#)].

[134] A. Mead, S. Brieden, T. Tröster and C. Heymans, *HMcode-2020: Improved modelling of non-linear cosmological power spectra with baryonic feedback*, [2009.01858](#).

- [135] J. S. Bagla and T. Padmanabhan, *Evolution of gravitational potential in the quasilinear and nonlinear regimes*, [astro-ph/9503077](#).
- [136] K. Kohri and T. Terada, *Semianalytic calculation of gravitational wave spectrum nonlinearly induced from primordial curvature perturbations*, *Phys. Rev. D* **97** (2018) 123532, [[1804.08577](#)].
- [137] K. N. Ananda, C. Clarkson and D. Wands, *The Cosmological gravitational wave background from primordial density perturbations*, *Phys. Rev. D* **75** (2007) 123518, [[gr-qc/0612013](#)].
- [138] D. Baumann, P. J. Steinhardt, K. Takahashi and K. Ichiki, *Gravitational Wave Spectrum Induced by Primordial Scalar Perturbations*, *Phys. Rev. D* **76** (2007) 084019, [[hep-th/0703290](#)].
- [139] R. Saito and J. Yokoyama, *Gravitational wave background as a probe of the primordial black hole abundance*, *Phys. Rev. Lett.* **102** (2009) 161101, [[0812.4339](#)].
- [140] R. Saito and J. Yokoyama, *Gravitational-Wave Constraints on the Abundance of Primordial Black Holes*, *Prog. Theor. Phys.* **123** (2010) 867–886, [[0912.5317](#)].
- [141] E. Bugaev and P. Klimai, *Induced gravitational wave background and primordial black holes*, *Phys. Rev. D* **81** (2010) 023517, [[0908.0664](#)].
- [142] K. Inomata, M. Kawasaki, K. Mukaida, Y. Tada and T. T. Yanagida, *Inflationary primordial black holes for the LIGO gravitational wave events and pulsar timing array experiments*, *Phys. Rev. D* **95** (2017) 123510, [[1611.06130](#)].
- [143] K. Ando, K. Inomata and M. Kawasaki, *Primordial black holes and uncertainties in the choice of the window function*, *Phys. Rev. D* **97** (2018) 103528, [[1802.06393](#)].
- [144] G. Janssen et al., *Gravitational wave astronomy with the SKA*, *PoS AASKA14* (2015) 037, [[1501.00127](#)].
- [145] A. Weltman et al., *Fundamental physics with the Square Kilometre Array*, *Publ. Astron. Soc. Austral.* **37** (2020) e002, [[1810.02680](#)].
- [146] J. Garcia-Bellido, H. Murayama and G. White, *Exploring the early Universe with Gaia and Theia*, *JCAP* **12** (2021) 023, [[2104.04778](#)].
- [147] A. Sesana et al., *Unveiling the gravitational universe at μ -Hz frequencies*, *Exper. Astron.* **51** (2021) 1333–1383, [[1908.11391](#)].
- [148] K. Schmitz, *New Sensitivity Curves for Gravitational-Wave Signals from Cosmological Phase Transitions*, *JHEP* **01** (2021) 097, [[2002.04615](#)].